Role of the $\mathbf{P_R}$ Intermediate in the Reaction of Cytochrome *c* Oxidase with O_2[†]

Joel E. Morgan,[‡,§] Michael I. Verkhovsky,[‡] Graham Palmer,[||] and Mårten Wikström*[,‡]

Helsinki Bioenergetics Group, Institute of Biotechnology, Biocenter 2 (Viikinaari 5), Room 2011, PB 56, University of Helsinki, FI-00014 Helsinki, Finland, and Department of Biochemistry and Cell Biology, Rice University, MS 140, Houston, Texas 77005-1892

Received February 5, 2001

ABSTRACT: The first discernible intermediate when fully reduced cytochrome *c* oxidase reacts with O_2 is a dioxygen adduct (compound **A**) of the binuclear heme iron−copper center. The subsequent decay of compound **A** is associated with transfer of an electron from the low-spin heme *a* to this center. This reaction eventually produces the ferryl state (**F**) of this center, but whether an intermediate state may be observed between **A** and **F** has been the subject of some controversy. Here we show, using both optical and EPR spectroscopy, that such an intermediate ($\mathbf{P_R}$) indeed exists and that it exhibits spectroscopic properties quite distinct from **F**. The optical spectrum of $\mathbf{P_R}$ is similar or identical to the spectrum of the $\mathbf{P_M}$ intermediate that is formed after compound **A** when two-electron-reduced enzyme reacts with O_2. An unusual EPR spectrum with features of a Cu_B(II) ion that interacts magnetically with a nearby paramagnet [cf. Hansson, Ö., Karlsson, B., Aasa, R., Vänngård, T., and Malmström, B.G (1982) *EMBO J. 1*, 1295−1297; Blair, D. F., Witt, S. N., and Chan, S. I. (1985) *J. Am. Chem. Soc. 107*, 7389−7399] can be uniquely assigned to the $\mathbf{P_R}$ intermediate, not being found in either the $\mathbf{P_M}$ or **F** intermediate. The binuclear center in the $\mathbf{P_R}$ state may be assigned as having an Fe_{a3}(IV)═O Cu_B(II) structure, as in both the $\mathbf{P_M}$ and **F** states. The spectroscopic differences between these three intermediates are evaluated. The $\mathbf{P_R}$ state has a key role as an initiator of proton translocation by the enzyme, and the thermodynamic and electrostatic bases for this are discussed.

Cytochrome *c* oxidase is a molecular energy transduction device. It catalyzes the reduction of dioxygen to water and converts the released energy into an electrochemical proton gradient ($\Delta\mu_{H^+}$)[1] that subsequently drives the synthesis of ATP. The enzyme requires four electrons and four protons to convert O_2 into water. These electrons and protons are transferred into the O_2 reduction site from opposite sides of the membrane, generating $\Delta\mu_{H^+}$. In addition, for each O_2 molecule reduced, the enzyme translocates four protons across the membrane, a process that doubles the efficiency of $\Delta\mu_{H^+}$ formation (*1*, *2*).

Reduction of O_2 to water takes place at a binuclear heme−copper site (Fe_{a3}−Cu_B). Electrons reach this site one at a time via two other metal centers, Cu_A and a low-spin heme (Fe_a). A number of catalytic intermediates have been observed in the reduction of O_2 to water (Figure 1). A detailed chemical description of these intermediates is crucial to understanding the catalysis of O_2 reduction and energy conservation (see refs *3* and *4*). Although the fully reduced enzyme contains four reducing equivalents, the reaction with O_2 can be started with two to four electrons in the enzyme. The simplest kinetics are found when the reaction begins with only two electrons, one on Fe_{a3} and one on Cu_B (Figure 1), and in this "mixed valence" case there is full agreement in the literature. Two intermediates are observed by optical spectroscopy. First, a species characterized by increased absorbance at 595 nm appears. The rate of this process depends on the O_2 concentration; at 1 mM O_2 the time constant (τ) is approximately 8 μs at room temperature (RT). This species was first identified and correctly assigned by Chance et al. (*5*) as a dioxygen adduct of Fe_{a3} in studies of the reaction at low temperatures, and the name "compound **A**", is still in use. Subsequently, this structure was clearly established by resonance Raman spectroscopy (see refs *2* and *3*). The second intermediate is characterized by an absorption peak at 607 nm. Again, the rate of appearance is dependent on O_2 concentration; $\tau \sim 170$ μs at 1 mM O_2 (*6*). This species was also originally identified at low temperatures by Chance et al. (*5*) and named "compound C", but it is now more often referred to as $\mathbf{P_M}$, where "**M**" indicates the **m**ixed valence or two-electron-reduced initial state of the enzyme prior to reaction with O_2. With the mixed valence enzyme the fast reactions stop at this point, and $\mathbf{P_M}$ can

[†] Supported by grants from the Academy of Finland, the University of Helsinki, the Sigrid Juselius Foundation, Biocentrum Helsinki, and the National Institutes of Health (GM 55807).

* Corresponding author. E-mail: Marten.Wikstrom@Helsinki.Fi. Telefax: +358-9-191 58001.

[‡] University of Helsinki.

[§] Current address: Department of Biochemistry, University of Illinois at Urbana-Champaign, A306 CLSL, Mail Code 25-6, 600 S. Mathews Ave., Urbana, IL.

[||] Rice University.

[1] Abbreviations: **A**, the ferrous dioxygen adduct of Fe_{a3}; $\Delta\mu_{H^+}$, electrochemical proton gradient; E_m, midpoint redox potential (vs NHE); **F**, ferryl intermediate of the oxygen reduction site; Fe_a, low-spin heme; Fe_{a3}, oxygen binding heme; *k*, rate constant; K_M, Michaelis constant; *N*-side, negatively charged side of the membrane; **O**, fully oxidized form of the oxygen reduction site; **P**, peroxy intermediate of the oxygen reduction site; *P*-side, positively charged side of the membrane; **R**, unliganded, fully reduced form of the oxygen reduction site; RT, room temperature; τ, time constant (1/*k*); TMPD, *N*,*N*,*N*′,*N*′-tetramethyl-*p*-phenylenediamine.

10.1021/bi010246w CCC: $20.00
Published on Web 05/15/2001

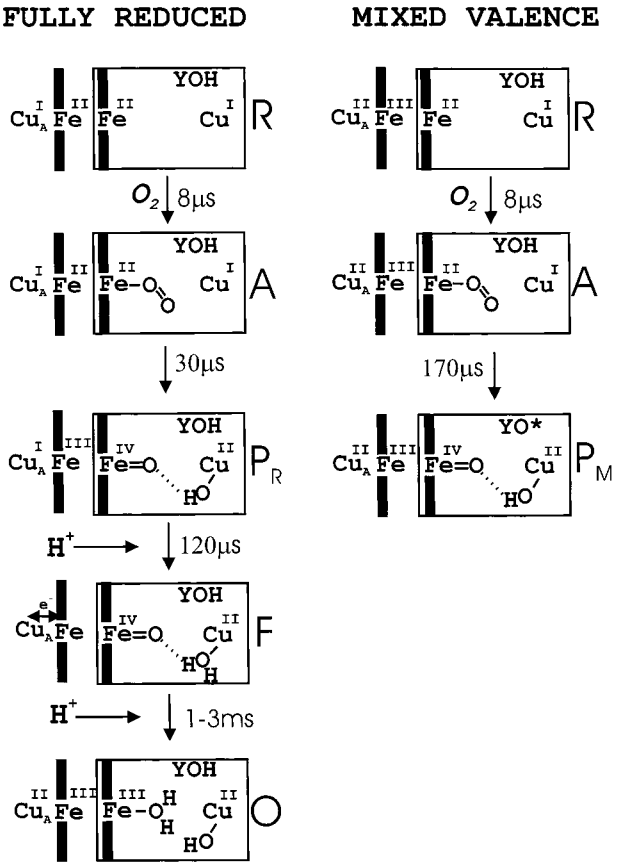

FIGURE 1: Intermediates in the reaction of cytochrome *c* oxidase with O_2. The scheme describes the structure of heme a_3 and Cu_B in the binuclear site (within the rectangle) and the redox states of the low-spin heme *a* and the Cu_A center (outside the rectangle) in the intermediates of the reaction of the fully reduced and mixed valence enzyme with dioxygen, as observed by time-resolved spectroscopic techniques (see text). Approximate time constants (τ) are given, as observed with the bovine heart enzyme for each reaction at room temperature. Only the distal ligand of heme a_3 and an oxygenous ligand of Cu_B are shown. YOH depicts the conserved tyrosine residue (Tyr-244)[4] in the binuclear center, and YO* stands for the neutral tyrosine radical. Net proton uptake into the enzyme is also shown, as observed (see text). Note that the reaction proceeds in the same way for the first step but differs in the formation of the **P** states, where $\mathbf{P_R}$ has one more electron in the binuclear site than $\mathbf{P_M}$. $\mathbf{P_R}$ is not thought to be preceded by $\mathbf{P_M}$ when an electron is available in the low-spin heme (see text). If an electron becomes available when the binuclear site is in the in $\mathbf{P_M}$ state (right), it is thought to be converted into $\mathbf{P_R}$ (left) and subsequently to the **F** state. One more electron is required to convert **F** into the fully oxidized state **O**. At room temperature, the conversion of $\mathbf{P_R}$ into **F** occurs roughly simultaneously with equilibration of the remaining electron between Cu_A and the low-spin heme (see text).

persist for several seconds to minutes, perhaps until additional reducing equivalents enter the enzyme.

In resonance Raman studies of the mixed valence reaction, two distinguishable species are also observed, of which the first (**A**) exhibits a mode at 568 cm^{-1} due to the Fe−O_2 vibration (see refs *2* and *3*). Even though $\mathbf{P_M}$ was long thought to be a "**p**eroxy" intermediate, a recent Raman study has identified a mode at 804 cm^{-1} that was assigned to the second intermediate ($\mathbf{P_M}$) and which is indicative of an Fe(IV)═O structure and of a broken O−O bond (*6*). Subsequent Raman studies with the mixed isotope $^{16}O-^{18}O$ had indeed indicated that the O−O bond is broken in the 804 cm^{-1} species produced by hydrogen peroxide treatment of the enzyme (*7*). Substantiating this conclusion, isotopic tracer studies using $^{18}O_2$ have also shown that when $\mathbf{P_M}$ is formed from the mixed valence enzyme, $H_2{}^{18}O$ appears in solution (*8*). Today, it can be considered established that $\mathbf{P_M}$ is not a peroxy species, despite the fact that it may be produced by energy-dependent two-electron abstraction from the oxidized enzyme (*9*), by the reaction of two-electron-reduced enzyme with O_2 (*5*, *6*), or by H_2O_2 reacting with the oxidized enzyme (*7*, *10*−*13*). Instead, in the reaction starting with the mixed valence enzyme, the dioxygen has been reduced by four electron equivalents in this compound: two of these electrons are provided by heme iron, one from copper, and the fourth probably from a conserved tyrosine present in the binuclear site (*6*, *14*−*16*). Alternatively, the fourth equivalent might arise from oxidation of Cu_B to Cu(III), although, as yet, the trivalent state of copper has not been found in biological systems.

When, on the other hand, the reaction begins with the fully reduced (four-electron) enzyme, a longer time course is found with at least four kinetic steps (Figure 1). The reaction is agreed to proceed in the same way for the first step (formation of **A**), but subsequently it becomes more complicated and less well understood. The first clear difference is that the rate by which **A** disappears is much faster; at room temperature τ is about 30 μs at 1 mM O_2, i.e., 5−6 times faster than for the mixed valence enzyme (see refs *2* and *3*). Furthermore, the overall changes in optical absorbance that take place in this phase are quite different from the corresponding phase of $\mathbf{P_M}$ formation in the mixed valence enzyme (*5*). This difference appears to center on the fact that Fe_a is initially in the ferrous state in the fully reduced enzyme. Optical experiments have indicated that a large fraction of Fe_a becomes oxidized at the same time as **A** decays (*17*, *18*), and this was supported by the resonance Raman studies of Rousseau et al. (*19*), who concluded that the decay of compound **A** is accompanied by transfer of the electron in Fe_a to the binuclear center. Thus, the ready availability of an electron in Fe_a appears to be the source of the difference between the fully reduced and mixed valence reactions.

However, the actual nature of the heme−oxygen intermediate that is produced by this electron transfer has remained controversial. Optical spectroscopy at low temperatures (*20*) indicated that it was similar to the $\mathbf{P_M}$ intermediate, after accounting for the spectral change due to the oxidation of Fe_a, but clearly different from the subsequent ferryl state **F** that has an absorption maximum near 580 nm; this has since been confirmed at room temperature (*21*). Due to its similarity to $\mathbf{P_M}$, Morgan et al. (*20*) called this intermediate $\mathbf{P_R}$ since it derives from the fully **r**educed enzyme. However, Orii (*22*) could not detect a **P**-like intermediate by optical spectroscopy, and Han et al. (*23*) recently reported that the early oxidation of Fe_a, as measured by Raman spectroscopy, had the same or a similar time constant to the formation of the **F** intermediate, the latter being assigned on the basis of its oxygen isotope-sensitive Raman band at 786 cm^{-1}. Although both of these groups believed that a peroxy intermediate exists in the reaction initiated from the fully reduced enzyme, they concluded that it went undetected because the rate of its conversion into **F** greatly exceeds its rate of formation. On the other hand,

Ogura et al. (*24*) reported a mode at 804 cm^{-1} preceding that at 786 cm^{-1}, indicative a second ferryl intermediate similar to $\mathbf{P_M}$ in structure, between the **A** and **F** states.

The major difficulty in detecting a **P**-like intermediate by optical spectroscopy in the O_2 reaction of the fully reduced enzyme is that while formation of such a state is expected to produce an *increase* in absorption at 607 nm, the simultaneous oxidation of Fe_a causes an absorption *decrease* of comparable magnitude at 605 nm.

Because of the oxidation of Fe_a, the binuclear center contains an additional reducing equivalent in $\mathbf{P_R}$ relative to $\mathbf{P_M}$, just as is the case for the ferryl intermediate **F**. In contrast to $\mathbf{P_M}$, the $\mathbf{P_R}$ intermediate is unstable and decays into the ferryl state **F** with no further electron transfer into the site. Accordingly, there should be *two* different oxygen intermediates of the binuclear center at the three-electron-reduced level, viz. $\mathbf{P_R}$ and **F**, with very different optical spectra.

A three-electron-reduced intermediate is expected to have unpaired spins and to exhibit EPR signals due to the presence of an odd number of unpaired electrons. On the basis of this expectation Hansson et al. (*25*) looked for, and found, a new copper signal for a three-electron intermediate in the O_2 reaction. This signal, which was extremely hard to saturate, exhibited only the $g_{||}$ feature and could be assigned to Cu_B(II) on the basis of the magnitude and location of the four-line hyperfine splitting due to the $I = {}^3/_2$ copper nucleus. The authors concluded that the intermediate in which the signal was seen corresponds to the second intermediate in the reaction of fully reduced enzyme with O_2 (the first being compound **A**), that the O−O bond has been broken in this state, and that Fe_{a3} is in a ferryl form. A magnetic interaction between Cu_B(II) and the ferryl iron was proposed to be the reason for the unusual properties of the EPR signal. Repeating the reaction with $^{17}O_2$ produced a broadening of this signal, which was attributed to bonding of one of the two oxygen atoms as an OH^- ligand of Cu_B (*25*). This remarkable conclusion from 1982 is precisely in line with present thoughts (see below), and it may be of historical interest to trace why it was neither pursued by the Göteborg group nor generally adopted by the scientific community. One possible reason is that this intermediate was usually thought to be identical to the **F** intermediate (*26*, *27*), although Blair et al. (*28*) had made the important discovery in low-temperature experiments that there are *two* intermediates at the three-electron-reduced level and that only the first of these exhibits the unusual EPR signal.

The latter authors (*28*) found that the unusual Cu_B EPR signal decayed with no further electron transfer into the binuclear center. The temperature dependence of this process indicated that it was entropically promoted. In agreement with Hansson et al. (*25*), they concluded that the unusual EPR signal comes from an intermediate with three electrons in the binuclear site, in which Cu_B(II) interacts with a second paramagnet (*28*). However, their results indicated that this was only the first of *two* three-electron intermediates, the second of which was apparently EPR silent. They suggested that the EPR-active intermediate has a ferrous a_3−peroxy/cupric structure while the subsequent intermediate was a ferryl species. The possibility that the Cu_B signal came from a ferrous−cupric state had been ruled out by Hansson et al. (*25*), because they believed a ferrous−peroxy state of the heme iron to be low spin and hence diamagnetic, but faced with two intermediates to assign, Blair et al. (*28*) argued that a peroxide bridge between Fe_{a3} and Cu_B could make the bonding to Fe_{a3} sufficiently weak to promote a high or intermediate spin, and thus a paramagnetic state of the ferrous iron.

Unfortunately, neither of these studies was accompanied by detailed optical data that would enable a straightforward assignment of the unusual EPR signal to one of the known reaction intermediates. For these reasons, and due to the importance of intermediate $\mathbf{P_R}$, we have carried out low-temperature "triple-trapping" measurements (see ref *5*) in conditions where comparable samples could be observed by both optical absorption and EPR spectroscopy, as well as additional optical studies at room temperature. The results allows us to firmly conclude that $\mathbf{P_R}$ is a true intermediate in the reaction of the fully reduced enzyme with O_2 and to unambiguously assign the unusual EPR signal to this intermediate.

MATERIALS AND METHODS

Enzyme Preparation. Bovine heart cytochrome *c* oxidase was prepared by a modification of the procedure of Hartzell and Beinert (*29*). During purification the pH was kept above 7.8, and Triton X-114 and cholate were added on the basis of cytochrome aa_3 concentration rather than total protein (*30*). No ethanol was used to remove the Triton X-114 after the red/green cut; instead, the green pellet was repeatedly resuspended in the preparation buffer and centrifuged until the amount of detergent was significantly reduced, as judged by the extent of bubbling when the supernatant was shaken (not stirred; usually three to four exchanges).

Low-Temperature Kinetics. The triple-trapping method was devised by Chance and co-workers (*5*) as a way to slow the reaction of cytochrome oxidase with O_2 sufficiently for it to be studied by EPR and optical spectroscopy. In this method the reaction is photoinitiated and runs at about −100 °C. As the name implies, the method relies on a series of steps to "trap" the enzyme in certain states. First, the reduced enzyme, inhibited by CO, is cooled to about −20 °C in a water−antifreeze solution (ethylene glycol or glycerol). At this temperature, in the dark, the off-rate for CO is very small, and O_2 can be added without starting the reaction. After O_2 is added, the sample can be further cooled to −80 to −100 °C, where it is essentially stable in the dark. The reaction of the enzyme with O_2 can be initiated by removing CO with a flash of light. At this point the reaction can either be monitored spectrosopically in real time or frozen for study by methods such as EPR spectroscopy.

In a variation of this procedure that was used for the EPR samples, the reaction can be carried out by freezing the CO-bound enzyme/O_2 sample to liquid nitrogen temperature, photolyzing the CO at that temperature, and then running the reaction forward by briefly raising the temperature by plunging the samples into baths adjusted to higher temperatures (*31*).

Low-Temperature Optical Measurements. The samples had to be in the form of a low-temperature glass because our multiwavelength detection requires that the light emerging from the cuvette be reimaged so that it can be dispersed by the polychromator. It also had to be possible to cool the apparatus before samples were placed in it and then to

transfer prefrozen samples into the apparatus without warming. The temperature was maintained using a Dewar flask from a Shimadzu low-temperature spectrophotometer accessory. This Dewar has optical windows on two opposite faces and is equipped with nozzles that direct dry nitrogen onto the windows to prevent fogging. Instead of filling the flask with liquid nitrogen, an internal atmosphere of cold N_2 gas was used. Cooling was achieved by flowing N_2 gas through a copper coil immersed in liquid nitrogen. The cold gas was brought in through a foam block at the top of the Dewar and carried to the bottom by a length of tubing. The temperature was measured using a Pt resistor (Lakeshore Cryogenics) placed next to the sample cuvette at the same level in the Dewar. The temperature was adjusted by varying the flow of nitrogen gas into the system. The part of the apparatus above the top of the Dewar was enclosed in a plastic bag filled by a steady stream of dry N_2. This made it possible to change sample without the windows of the sample cuvette becoming frosted.

Spectrophotometric measurements were made using a diode array system (Unisoku, Kyoto). Fiber optic cables carried the light from the source to the sample and from the sample to the detector. At the sample Dewar cylindrical optical "heads", holding the end of the optic fiber and a lens, were positioned on opposite sides so that the light beam passed through the sample cuvette positioned at the center of the Dewar. Adjustable laser mounts (ULM-TILT, Newport) were used to fine-tune the alignment of the optical heads. Optical filter holders and a camera shutter were located between the light source and the input of the first optic cable. The polychromator also has a built-in shutter.

The system was initially cooled with an empty sample cuvette in the chamber; after the desired temperature was reached, a reference sample made from glycerol, buffer, and detergent was made in the form of a low-temperature glass by plunging the cuvette into liquid nitrogen and loaded into the Dewar. To avoid frosting of the cuvette windows, the cuvette, still in liquid N_2, was brought into the plastic bag at the top of the Dewar. The sample cuvette could be removed from the liquid N_2 under a dry N_2 atmosphere and inserted into the Dewar without building up any condensation.

Enzyme Samples. Cytochrome *c* oxidase samples were initially prepared on a vacuum line. Samples were first made air-free, and then ascorbate, TMPD, and CO were added. Next, air-free (nitrogen-purged) glycerol was added using a gastight syringe (Hamilton), and the sealed sample was cooled to −20 °C in a thermostated bath. Meanwhile, an O_2-saturated solution was prepared by slowly bubbling O_2 gas through a glycerol/buffer solution previously cooled to −20 °C. The ambient light level was then decreased considerably; a volume of the O_2-saturated solution was added to the enzyme sample, and the mixture was loaded into the cuvette, which was then plunged into liquid N_2; the sample was then transferred to the measurement Dewar as described above. After the sample was loaded, there was a delay of some minutes in order to allow the temperature and the glassy state of the sample to stabilize. To ascertain that a stable glass had been formed, the light transmission level was checked, using a 650 nm cutoff filter to prevent premature photolysis. Once the system was stable, the reaction was initiated using a xenon camera flash as follows: The probe beam shutter was first opened and data acquisition with the diode array begun. After a delay to allow one or two prephotolysis spectra to be acquired, a shutter at the detector was closed momentarily while the sample was photolyzed by a camera flash and then reopened.

Samples for EPR Spectroscopy. The initial preparation was the same as for optical samples. At −20 °C, the fully reduced enzyme CO adduct was mixed with O_2-saturated buffer, loaded into precooled EPR tubes, and frozen into liquid N_2. Photolysis was accomplished by placing the EPR tubes in a finger Dewar and illuminating the sample with a quartz halogen lamp for several minutes. The light beam passed through several centimeters of water to prevent heating. After photolysis at 77 K, the reaction was allowed to progress for short intervals of time by taking the sample out of liquid N_2 and plunging it into a bath of ethanol at −90 °C. Since the sample does not reach this temperature immediately, the real time of the reaction at −90 °C was measured using a thermocouple and used when plotting the kinetic data of Figure 4. Typically, for each reaction "step" the samples were left in the ethanol bath for 20 s at a time. At any time between reaction steps the samples could be placed in the EPR cryostat and the EPR spectrum recorded. The EPR spectra were run on a Bruker Model ESP 300 X-band spectrometer equipped with an Oxford cryostat.

Optical studies at room temperature were performed as described (*32*).

Data analysis was carried out using MATLAB and SPLMOD, a global multiexponential fitting program (*33*).

RESULTS AND DISCUSSION

Low-Temperature EPR and Optical Data. Figure 2 shows EPR spectra of cytochrome *c* oxidase trapped by low temperature during the course of the reaction of the fully reduced enzyme with O_2. The sample was prepared by photodissociating CO from the enzyme at 77 K in the presence of O_2, after which the reaction was allowed to proceed forward in short steps by briefly warming the sample to −90 °C (see Materials and Methods). These example spectra were acquired after the reaction had proceeded for 150 s. At this point, the unusual Cu_B signal is clearly visible (Figure 2, trace a), exhibiting the characteristic four-line spectrum ascribed to $g_{||}$ of Cu_B(II) (*25*, *28*, *34*). This spectrum was recorded at high microwave power (200 mW) and 4.9 K, under which conditions the other EPR signals associated with cytochrome *c* oxidase are almost completely saturated. However, one can nevertheless detect signs of the $g = 3$ signal from ferric low-spin Fe_a and a residual of the $g \sim 2$ signal from the oxidized Cu_A center. These other signals can be observed much more clearly at lower microwave power (2 mW; Figure 2, trace b). To study the kinetics of the reaction, spectra were recorded at intervals thoughout the process; at each time point, in addition to the high-power spectrum, a spectrum was also recorded at 2 mW in order to follow the oxidation of Fe_a and Cu_A.

There are two unusual features in the EPR spectrum of Cu_B. First, it can only be detected at high microwave power and very low temperatures, implying that the unpaired electron can relax extremely efficiently. Second, only a small portion of the complete copper EPR is apparent; this consists of the more or less normal $g_{||}$ with hyperfine splitting of ca.

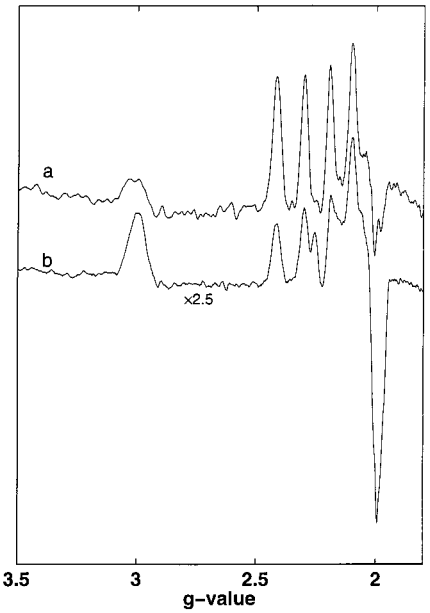

FIGURE 2: EPR spectrum of bovine heart cytochrome *c* oxidase 150 s after the start of the reaction of the fully reduced enzyme with O_2 at −90 °C. Sample (before mixing): 0.364 mM enzyme, 5 mM ascorbate, 25 μM hexammine ruthenium(II), 40% (v/v) glycerol, and 1% CO equilibrated at room temperature. Buffer containing 20 mM HEPES (pH 7.5) and 40% (v/v) glycerol was saturated with O_2 at −20 °C prior to mixing (mixing ratio 1:1). EPR parameters: microwave frequency 9.421 GHz, temperature 4.9 K, modulation amplitude 9.929 G, microwave power 200 mW (trace a) and 2 mW (trace b). Note that the prominent feature between the second and third Cu_B hyperfine lines at 2 mW (trace b) is due to the g_y transition from ferric heme *a*.

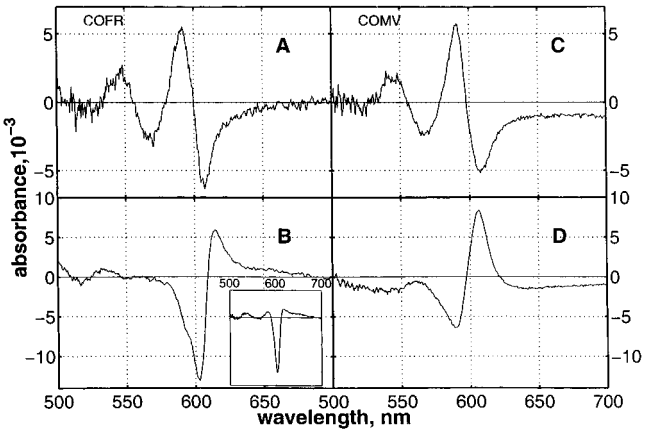

FIGURE 3: Spectra of kinetic components from the reaction of mixed valence (right panels) and fully reduced (left panels) cytochrome *c* oxidase with O_2 at −90 °C. (A and C) Spectra of the fast components with rate constants of 0.21 and 0.13 s^{-1}, respectively. (B and D) Spectra of the slow components with rate constants of 0.0245 and 0.0076 s^{-1}, respectively. The spectra were obtained by global multiexponential fitting of the data surface. Fully reduced enzyme (before mixing): 0.11 mM cytochrome *c* oxidase, 0.1% (w/v) dodecyl maltoside, 20 mM HEPES (pH 7.5), 40% (v/v) glycerol, 10 μM TMPD, 5 mM ascorbate, and saturated CO at room temperature. Mixed valence enzyme: The same conditions but without ascorbate and TMPD; after reaching the CO-liganded mixed valence state the CO concentration was dropped to 1%. Buffer containing 20 mM HEPES (pH 7.5) and glycerol 40% (v/v) was saturated with O_2 prior to mixing (mixing ratio 1:1). Inset: the result of subtracting the spectrum in (D) from that in (B).

140 G, centered at a *g*-value of 2.24. However, the absorption that would be expected to appear at $g_\perp = 2.04$ (*35*) is completely missing with only a trace residual contribution due to Cu_A, and there is no apparent EPR contribution from the remainder of the Cu_B species over the range $g = 1-5$.

The *g*-value of the resonance which is observed ($g_{||} = 2.24$) is not unusual for the cupric ion (*36*, *37*). The $g_{||}$ value varies with the identity of the ligands, the geometry of the complex, and the net charge on the copper ion. Copper centers with 3N1O coordination have $g_{||}$ values in the range 2.22−2.27 and $A_{||}$ values in the range 160−190 G (*37*); tetrahedral distortions will decrease both of these parameters with $A_{||}$ being more sensitive to the distortion. Examination of the crystal structure model of azide-bound cytochrome oxidase (*38*) which has the best defined four-coordinate Cu_B, reveals a small but definite distortion of the coordination geometry away from square planar toward tetrahedral. One well-defined EPR spectrum of Cu_B is provided by the cyanide adduct of cytochrome ba_3 from *Thermus thermophilus* (*39*), which presumably has 4N coordination; here $g_{||} = 2.28$, $A_{||} = 140$ G. Thus the detectable features of the spectrum in Figure 2 fall well within the range characteristic of relevant coordination compounds, i.e., those compounds for which the deviation from square planar symmetry is modest, typically having a tetragonal or mild tetrahedral distortion.

The reactions of both fully reduced and mixed valence enzyme with O_2 were also followed by optical spectroscopy at −90 °C. The optical samples were made using the same buffer, detergent, and antifreeze/glassing agent used in the EPR samples in order to make the results from the two methods as closely comparable as possible (see Materials and Methods). A global exponential fit to the acquired optical data was used to extract the kinetic phases. The right-hand panel of Figure 3 show the spectra of the two kinetic components observed for the mixed valence enzyme. The first component ($\tau = 7.6$ s; panel C) shows a decrease in absorbance just above 600 nm, reflecting the disappearance of the unliganded reduced Fe_{a3}. This is accompanied by an absorption increase at ∼592 (α-band) and ∼550 nm (β-band), which reflects formation of the ferrous−oxygen adduct of Fe_{a3}, i.e., compound **A** (cf. ref *5*). The second component ($\tau = 132$ s; panel D) shows a decrease of absorbance near 592 nm reflecting the decay of compound **A**, which is accompanied by an increase above 600 nm due to formation of the $\mathbf{P_M}$ intermediate.

The results for the fully reduced enzyme are shown in the left-hand panels of Figure 3. The first kinetic component is similar in rate ($\tau = 4.7$ s; panel A) and spectrum to the corresponding component for the reaction of the half-reduced enzyme. However, the second component is formed more quickly ($\tau = 40.8$ s; panel B) and has a significantly different spectrum. These results are very similar to those reported previously in measurements run at −25 °C (*20*). The spectrum of the second phase is what would be expected if conversion of intermediate **A** to **P** in the reaction of the fully reduced enzyme is accompanied by oxidation of low-spin Fe_a. In fact, this spectrum can be quantitatively accounted for as the sum of oxidation of the low-spin Fe_a, which causes a decrease of absorbance just above 600 nm, and the decay of the **A** intermediate into $\mathbf{P_M}$ in the mixed valence case already described (panel B, inset). Thus, $\mathbf{P_R}$ and $\mathbf{P_M}$ give rise to similar, or identical, optical spectra of the binuclear

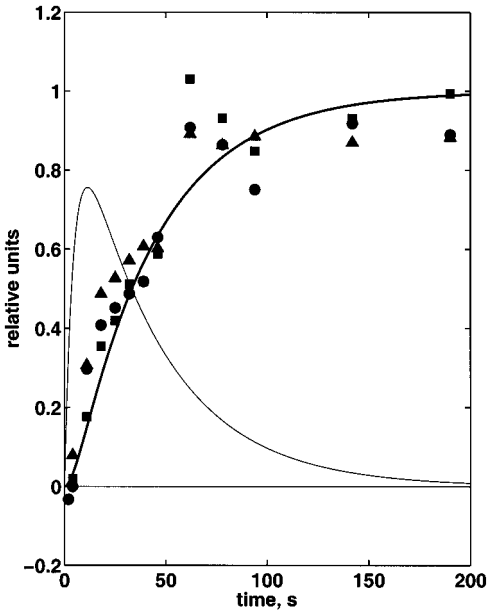

FIGURE 4: Time course of the reaction of fully reduced cytochrome *c* oxidase with O_2 at −90 °C. Thin curve: formation and decay of compound **A**> Thick curve: formation of state $\mathbf{P_R}$. The two curves were obtained by simulating the reaction using the rate constants obtained from a global fit of the data from Figure 3 using the rate constants 0.214 s^{-1} and 0.0245 s^{-1} (see text). Symbols: (■) intensity (arbitrary units) of the $g = 3$ EPR signal of oxidized Fe_a; (●) intensity (arbitrary units) of the unusual EPR signal from Cu_B.

site, even though this site contains one additional electron in the $\mathbf{P_R}$ state.

The reaction of the fully reduced enzyme with O_2 was modeled as two sequential reactions, using the time constants obtained by fitting the optical data ($\tau_1 = 4.7$ s and $\tau_2 = 40.8$ s) and following the simple reaction scheme:

$$\mathbf{R} \xrightarrow{\tau_1} \mathbf{A} \xrightarrow{\tau_2} \mathbf{P_R}$$

The time course of intermediates **A** and $\mathbf{P_R}$ calculated in this way are shown as thin and thick solid curves, respectively, in Figure 4. The squares show the time course of the intensity of the $g = 3$ EPR signal due to ferric Fe_a, and the circles show the relative amplitude of the unusual EPR signal from Cu_B. The $g \sim 2$ signal from oxidized Cu_A was found to rise with the same time course as the appearance of ferric Fe_a (not shown; cf. ref *28*). Thus, at low temperatures, Fe_a equilibrates electronically with Cu_A within the time span of the decay of intermediate **A**. This is in contrast to the case at room temperature where this equilibration has been found to take place later, viz. during the reaction step $\mathbf{P_R} \rightarrow \mathbf{F}$ (see below).

From these results it is clear that the unusual Cu_B signal rises together with the oxidation of Fe_a, as monitored by EPR spectroscopy, and that both of these processes correspond temporally to the formation of the $\mathbf{P_R}$ intermediate, as measured optically.

The unusual EPR signal was also observed in an experiment with the mixed valence enzyme reacting with O_2, but the maximum amplitude of this signal was only 6−7% of that observed with the fully reduced enzyme. Since this would be expected if the enzyme in the mixed valence sample was reduced slightly beyond the two-electron level—a common occurrence, we conclude that the unusual EPR signal is not present in the $\mathbf{P_M}$ state.

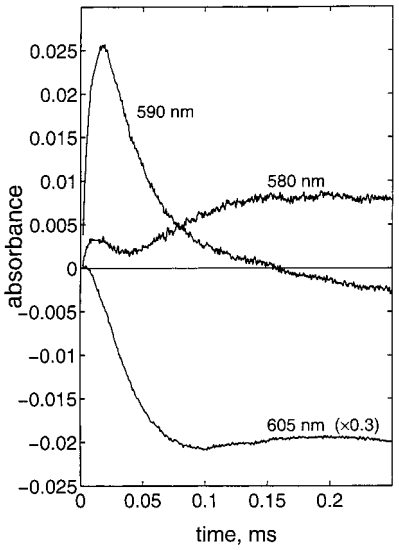

FIGURE 5: The reaction of the fully reduced cytochrome *c* oxidase with O_2 at room temperature. The reaction starts by a laser flash, but the absorbance change due to photolysis has been subtracted from the data. Concentrations after mixing: 6.4 μM enzyme, 1 mM O_2, 100 mM MES buffer (pH 6), and 0.1% dodecyl maltoside.

Room Temperature Kinetics. Figure 5 shows the time course of the reaction of fully reduced enzyme with O_2 at room temperature, measured at three different wavelengths. The **F** intermediate absorbs maximally at 580 nm while the absorption change due to formation of compound **A** may be followed at 590 nm, a wavelength isosbestic for the redox change in Fe_a, which was measured at 605 nm. It is clear from these traces that the **F** intermediate is formed more slowly than either the oxidation of Fe_a or the decay of compound **A**, which both occur with similar kinetics. This strongly indicates that the $\mathbf{P_R}$ intermediate also exists at room temperature. Consistent with this, at 580 nm one can actually distinguish *three* phases in the early reaction: these are assigned as the binding of O_2 to generate **A**, conversion of **A** to $\mathbf{P_R}$, and formation of **F** from $\mathbf{P_R}$.

Figure 6 shows the initial time course of the reactions of fully reduced and mixed valence enzyme with O_2 in water and in D_2O buffer. After an initial downward jump in absorbance due to photolysis of CO, the rise in absorption reflects the formation of compound **A**. This phase has the same rate for the mixed valence and the fully reduced enzyme and is unaffected by solvent isotope substitution (cf. ref *40*). The subsequent decrease in absorption is due to the $\mathbf{A} \rightarrow \mathbf{P_M}$ (upper trace) and $\mathbf{A} \rightarrow \mathbf{P_R}$ transitions (lower trace), respectively, and confirms that the former is about 5 times slower than the latter (see introduction). In both cases the deuterium substitution slows down the rate by a factor of ca. 1.4, as also reported by Brzezinski et al. (*40*). It is known from previous studies that in neither case is there net uptake of protons from the medium (*41*, *42*) or translocation of protons perpendicular to the membrane dielectric (*43*). We conclude that formation of the **P** states from compound **A** is probably associated with the breaking of a hydrogen bond, independent of whether the reaction is accompanied by electron transfer from Fe_a to the binuclear site ($\mathbf{P_R}$) or not ($\mathbf{P_M}$).

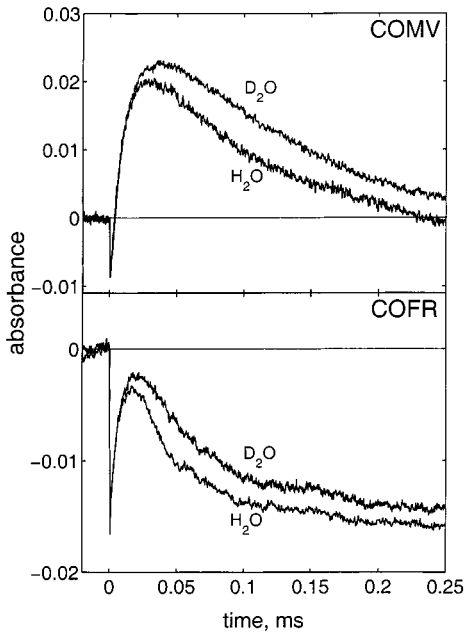

FIGURE 6: Solvent isotope effect on the early reactions of cytochrome *c* oxidase with O_2. Top panel: mixed valence enzyme, wavelength 595 nm. Bottom panel: fully reduced enzyme, wavelength 590 nm. Each kinetic trace is the average of 12 transients. Concentrations after mixing: 2.4 μM cytochrome oxidase, 50 mM HEPES (pH = 7 or pD = 7), 0.1% (w/v) dodecyl maltoside, 0.2 mM CO, and 1 mM O_2.

The Physiological Role of Fully Reduced Cytochrome c Oxidase. As discussed above, the $\mathbf{P_R}$ state has so far been observed only in the reaction of the fully reduced enzyme with O_2. From time to time the contribution of the fully reduced enzyme in the catalytic cycle of cytochrome *c* oxidase has been questioned, because its occupancy during turnover is very low under most aerobic experimental conditions. However, even in normoxic tissues the local O_2 concentration may be 2 orders of magnitude lower than that of typical air-saturated buffers used experimentally (*44*). Gnaiger et al. (*45*) have recently shown that the efficiency of oxidative phosphorylation is actually increased under hypoxic conditions where the O_2 concentration was lower than the apparent K_M for O_2; under such conditions the fully reduced enzyme will almost certainly be a substantially occupied intermediate. In agreement with this, we have recently reported that the energy-conserving efficiency of cytochrome *c* oxidase is not decreased by initiating the reaction from the fully reduced state (*46*).

Structure of $\boldsymbol{P_R}$. The data presented here show unequivocally that $\mathbf{P_R}$ is a distinct intermediate state of the binuclear center in the reaction of the fully reduced enzyme with O_2 at both room temperature and low temperature, which confirms the early proposal that this reaction, like that of the mixed valence enzyme, also takes place via a **P**-like species (*9*, *47*). $\mathbf{P_R}$ is formed from the **A** state in a reaction that is coupled to the transfer of a single electron to this center, and it subsequently decays to the ferryl **F** state with no further electron input (cf. ref *28*). In collaboration with Ludwig and co-workers we have studied the same reaction in a bacterial relative of cytochrome *c* oxidase, viz. the cytochrome ba_3 quinol oxidase from *Paracoccus denitrificans* (*48*). In this case, the low-spin heme is a protoheme (heme *b*) and does not complicate the absorption changes due to oxygen intermediates in the 600 nm band. In agreement with the present results, we indeed detected an absorption increase at 607 nm concomitant with oxidation of the low-spin heme of this enzyme at room temperature, when the fully reduced state reacted with O_2 (manuscript in preparation).

Our results show that the unusual EPR signal can be uniquely assigned to the $\mathbf{P_R}$ intermediate, and this establishes a cupric Cu_B for this state. In their original report, Karlsson et al. (*34*) pointed out that the unusual behavior of the EPR signal is suggestive of spin coupling between the iron of heme a_3 and Cu_B. Subsequently, Hansson et al. (*25*) showed that the copper hyperfine lines were broadened when $^{17}O_2$ was used as oxidant. The magnitude of this broadening was consistent with the presence of a single oxygen derived from O_2 in the coordination sphere of Cu_B. They suggested that the EPR spectrum was due to a coupled Fe(IV)═O···HO—Cu(II) spin system and noted that the observed behavior was inconsistent with strong magnetic coupling ($J \gg D$; see below) but could be explained if $J \approx D$. In contrast, Blair et al. (*28*) subsequently suggested that the anomalous EPR spectrum was due to a peroxide-bridged structure and explored the possibility of coupling between the Cu_B(II) and a peroxy form of Fe_{a3}(II), with the latter having an integer spin of either 1 or 2. However, it has since been established, mainly by resonance Raman spectroscopy, that the heme iron is in the ferryl form in both the **F** and the $\mathbf{P_M}$ states of the binuclear site (see introduction). Judging from the close similarity, or identity, between the optical spectra of $\mathbf{P_R}$ and $\mathbf{P_M}$, and the fact that the optical spectrum derives mostly from the Fe_{a3} heme, it seems very likely that this heme is also in the ferryl form in $\mathbf{P_R}$, a conclusion that is supported by the Raman data of Ogura et al. (*24*).

The weak coupling between the $S = 1$ ferryl heme and the $S = {}^1/_2$ cupric ion results in the formation of six magnetic states that are split into three doublets. The behavior of this coupled system is determined by two parameters. The first is *J*, the parameter quantifying the coupling between the two spins,[2] and the second is *D*, the axial zero-field splitting of the $S = 1$ ferryl ion. In the enzymes and model compounds that have been characterized, the value of *D* for the $S = 1$ ferryl state falls in the range of 20−30 cm^{-1} (*49*−*53*), with the lower values being observed when imidazole is the proximal ligand to the heme. For positive *D* the lowest doublet has an effective spin of $^1/_2$ regardless of the sign of *J*, which can be either positive or negative. Negative values for *J* imply ferromagnetic coupling between the two spins, and this can be rejected because $g_\perp$ would fall in the range 2−4.5, the latter value being approached asymptotically with increasing values of the ratio *J*/*D* (*52*, *53*). However, since no additional EPR signal was observed in this range of *g*-values, ferromagnetic coupling can be unequivocally eliminated and the coupling must be antiferromagnetic.

The consequences of coupling between $S = 1$ and $S = {}^1/_2$ paramagnets have been developed quantitatively by Bencini and Gatteschi (*54*), by Hulliger (*55*), and by Hansson and Vänngård.[3] Figure 7 presents graphically the behavior of $g_\perp$, $g_\parallel$, and $A_\parallel$ as the ratio *J*/*D* is varied over a large range.[3] The two striking features of this figure are the relative constancy

[2] *J* is defined via the Hamiltonian $S_1 \cdot J \cdot S_2$, where S_1 and S_2 are the spin states of Fe and Cu. In this convention a positive *J* implies antiferromagnetic coupling.

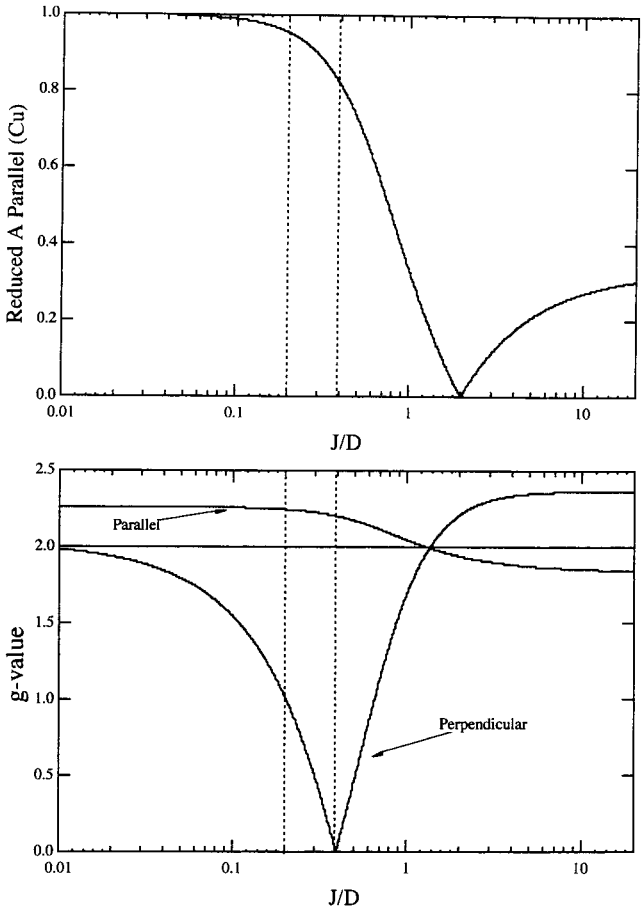

FIGURE 7: Behavior of the EPR parameters of a coupled $S = 1$ Fe(IV)=O center with $S = {}^1/_2$ Cu(II) as a function of the ratio of the exchange coupling $(J)^2$ to the zero-field splitting of the iron center (D). Upper panel: The fractional reduction in the size of the *z*-component of the copper hyperfine coupling. Lower panel: The variation in $g_{||}$ and $g_\perp$. The curves were calculated using the solutions published by Hulliger (*55*) assuming the following parameters for the uncoupled species: Cu(II), $g_{||} = 2.26$, $g_\perp = 2.03$ (*52*); Fe(IV), $g_{||} = 2.28$, $g_\perp = 1.94$ (*37*). The solutions assume that the rhombic component of the zero field splitting is small and that the exchange interaction is isotropic.

of both $g_\perp$ and $g_{||}$ as long as J/D is <0.1 and >1 and the dramatic decrease in $g_\perp$ when J/D goes above 0.1, passing through zero when J/D is about 0.4.

Given that the values observed here for $g_{||}$ and $A_{||}$ are within the range normally observed for cupric ion and that there is significant EPR intensity at $g_{||}$, the upper limit on J/D must be significantly less than indicated by the vertical dashed line on the right (Figure 7). Furthermore, the absence of any EPR signal due to $g_\perp$ at magnetic fields up to 6600 G implies that $g_\perp < 1$, and this sets the lower level on J/D as shown by the vertical dashed line on the left (Figure 7). It would thus appear that the two metals are coupled antiferromagnetically, that J/D is 0.2−0.4, and thus that J is approximately 4−8 cm^{-1}, which agrees with the values deduced by Hansson et al. (*25*).

Another possibility is that the $g_\perp$ feature is too broad to be observed due to a spread of *J*-values. A distribution in the magnitude of coupling was considered early in the characterization of the EPR of compound I of the peroxidase family of enzymes (*53*). Here, exchange coupling occurs between the $S = 1$ ferryl state of the heme iron and the porphyrin π-cation radical. The nature of this coupling is very sensitive to distortions of the porphyrin. In planar porphyrins the interaction is ferromagnetic. As the symmetry of the porphyrin skeleton is reduced, typically by a buckling, the likelihood of overlap between the magnetic orbitals of the two participants increases and antiferromagnetic behavior becomes possible. Thus, in this system, both the size and the sign of J are a sensitive function of the conformation of the porphyrin. For chloroperoxidase, one case that has been thoroughly examined, it was found that J is positive and that a small variation in J (ca. 2% of the absolute value) improved the ability of simulations to fit the recorded spectrum (*52*).

By taking the derivative of the curves in Figure 7, it was found that the maximum sensitivity of $g_\perp$ to such a distribution of *J*-values occurs when J/D is about 0.2, i.e., when $g_\perp$ is already less than 1. The slope of the derivative at this point is 1, and thus a spread in *J*-values comparable to that invoked for chloroperoxidase would lead to only a 2% spread in $g_\perp$. We believe that a variation of this magnitude is insufficient to explain the absence of the $g_\perp$ feature by broadening due to a distribution of *J*-values.

We conclude that $\mathbf{P_R}$ and $\mathbf{P_M}$ are similar insofar as they both have a ferryl Fe_{a3}. Since the binuclear site has one more oxidizing equivalent in $\mathbf{P_M}$ [a neutral tyrosine radical or Cu_B(III); see introduction], the difference between $\mathbf{P_R}$ and $\mathbf{P_M}$ can be assigned to the fact that the former obtains the additional electron from Fe_a, while in the latter this electron derives from the tyrosine or Cu_B within the binuclear site However, the tyrosine radical [or Cu_B(III)], i.e., the $\mathbf{P_M}$ state, is probably never formed in the reaction of the fully reduced enzyme with O_2. Instead, the electron from Fe_a may be transferred directly in a rate-limiting step to an putative, unstable peroxy state before scission of the O−O bond (*56*). This is in contrast to the view of Sucheta et al. (*21*) that the decay of compound **A** leads to a 1:1 equilibrium mixture of the structural equivalents of compounds $\mathbf{P_M}$ and $\mathbf{P_R}$ (which they called P and F_o and where they assigned an **F**-like spectrum for F_o). However, our finding that the electron tunneling rate between Fe_a and the binuclear site is a determinant of the rate by which compound **A** is transformed into $\mathbf{P_R}$ (*57*) supports the notion that $\mathbf{P_M}$ is never formed in the reaction of the fully reduced enzyme with O_2 (see also ref *58*).

Structure of F. The **F** state has also been assigned as a ferryl−cupric form of the binuclear site (see introduction), and the question emerges why both its EPR and optical spectra differ so drastically from those of $\mathbf{P_R}$ (and $\mathbf{P_M}$). As suggested by several workers (*6*, *15*, *59*, *60*), this may be attributed at least partially to the additional proton in **F**, which may reside near the binuclear center. Our analysis (Figure 7) suggests a mechanism whereby the EPR spectrum of $\mathbf{P_R}$ could easily disappear in the **F** state. If the magnitude of the exchange coupling approximately doubles in the transition from $\mathbf{P_R}$ to **F**, as a consequence of even a subtle change in the structure at the binuclear center, the effect would be to make $g_\perp$ approximately zero. Since the transition probability for EPR absorption associated with a specific *g*-value is proportional to the mean of the other two *g*-values (*61*), the

[3] Örjan Hansson and Tore Vänngård (Department of Biochemistry and Biophysics, Chalmers Technical University and Göteborg University, Sweden) have independently performed calculations similar to those presented here and obtained the same result (unpublished).

transition probability at $g_{||}$ becomes extremely small when $g_{\perp}$ is close to zero, and thus no EPR signal would be detected at any location over the range 0−6600 G. Viewed in this light, it may be considered remarkable that an EPR signal is observed at all from this system.

The nature of the structural change can only be surmised at this time. However, the transition of either $\mathbf{P_M}$ (*42*, *62*) or $\mathbf{P_R}$ (*41*) to **F** is associated with the net uptake of one proton into the enzyme. There are three plausible candidates near the active center for the group that binds this proton. These are Glu-242,[4] Tyr-244,[4] and the hydroxide ion that is coordinated to Cu_B. Neutralizing a negative charge of any of these moieties could profoundly modify the strength of the antiferromagnetic coupling between Fe_{a3} and Cu_B. The OH^- ligand of Cu_B is by far the closest and thus most able to affect magnetic coupling between the binuclear site metals, making it the most likely candidate. It seems quite plausible that an OH^- ligand of Cu_B(II) in the $\mathbf{P_R}$ state (*25*) becomes protonated to an aquo ligand in **F** with enhanced hydrogen bonding (and spin coupling) between Cu_B and the oxygen of the ferryl iron (Figure 1). Such a protonation may also be sufficient to explain the dramatic change in the α-band of the optical spectrum (*6*, *60*), while the Soret spectrum remains essentially the same for these two intermediates, as well as for $\mathbf{P_M}$ (*11*, *12*).

Kinetic Isotope Effect. The conversion of intermediate **A** to **P** is slowed in D_2O buffer by a factor of about 1.4 irrespective of whether the reaction is accompanied by transfer of the third electron into the binuclear center. This deuterium isotope effect may be attributed to a local proton transfer in the process that precedes the scission of the O−O bond and which may be the same during formation of both $\mathbf{P_M}$ and $\mathbf{P_R}$ (*56*). It should be recalled that neither reaction is associated with net proton uptake into the enzyme or with generation of membrane potential (*41*−*43*). The faster rate of formation of $\mathbf{P_R}$, relative to $\mathbf{P_M}$, might be attributed to a somewhat lower activation barrier in forming the ferric−peroxy transition state prior to the scission of the O−O bond. Indeed, the electron tunneling rate has been shown to be a determinant of the rate of formation of $\mathbf{P_R}$ (*57*). It is possible, therefore, that the oxidation of Fe_a has already taken place during formation of the transient peroxy state (see ref *56*).

Rate of Cu_A/Fe_a Equilibration. It is interesting to note that, in general, the reaction of cytochrome *c* oxidase with O_2 follows a route at low temperatures very similar to that at room temperature, thus validating the use of the triple-trapping technique (*5*) to gain insight in the reaction. However, there are some apparent differences, and the timing of the rereduction of Fe_a by Cu_A may be of special interest. At room temperature, this has been described to occur concomitant with the conversion of $\mathbf{P_R}$ to **F** ($\tau \sim 125$ μs at pH 7.4; see ref *3*), but at −90° it clearly occurs synchronously with the oxidation of Fe_a and the *fomation* of $\mathbf{P_R}$ (cf. ref *28* and above). Thus, it appears that the rates of either $\mathbf{P_R}$ formation from **A** or its decay to **F**, or both, are slowed more by low temperature than the electron equilibration between Cu_A and Fe_a. This may well be related to the fact that both former reactions are proton coupled (*40*; Figure 6), whereas the latter is not (*63*). The apparent late oxidation of Cu_A by Fe_a in the oxygen reaction at room temperature, relative to the known rate of electron equilibration between these sites (*64*, *65*), has been ascribed to a requirement that the binuclear site be protonated to raise the E_m of Fe_a sufficiently (*66*, *67*). It is possible that at −90° the E_m of Fe_a is higher than that of Cu_A already without this protonation.

Role of P_R in Proton Pumping. The notion of electroneutrality at the binuclear center has been stressed, particularly by Rich (*68*) but also in other proposed mechanisms of proton translocation by cytochrome *c* oxidase (*69*, *70*). We consider the driving force for proton translocation to arise from electron transfer into the binuclear site. This creates a base and a negative charge in that site, which leads to the loading of a proton pump site from the *N*-side of the membrane (cf. below). Next, a conformational switch would connect the pump site with the *P*-side of the membrane and open the binuclear site for protonation (*60*, *69*). Finally, a second proton is transferred from the *N*-side to the base at the binuclear site, and the proton in the pump site is expelled into the aqueous *P*-phase. Without speculating here on the chemical nature of the pump site (but see refs *60* and *69*), it is clear from such a scenario that the $\mathbf{P_R}$ intermediate is of particular interest. Its formation is associated with transfer of an electron from Fe_a to the binuclear site *without any evident charge compensation* of that site. Thus, the $\mathbf{P_R}$ state of the binuclear center may be considered a "high-energy" state, the decomposition of which will drive proton translocation. Indeed, the subsequent transformation of $\mathbf{P_R}$ into **F** is coupled to translocation of a proton across the membrane, net uptake of another proton into the binuclear site, and an accompanying generation of transmembrane electric potential (*43*, *71*). Interestingly, at low temperatures this reaction was shown to follow nonexponential kinetics and to be associated with a considerable positive entropy of activation (*28*). The latter might be attributed to breaking of bonds, displacement of residues, or a decrease in the solvation of charged reactants on forming the transition state. This would be consistent with the scenario described above where the negatively charged binuclear site in $\mathbf{P_R}$ attracts a proton from the aqueous *N*-side of the membrane and where the pump site needs to be switched from protonic contact with the *N*-side to contact with the *P*-side of the membrane. Nonexponential kinetics at low temperatures are often encountered in heme proteins and have been explained as due to multiple, noninterconvertible conformational states with a distribution of activation energies (*72*). The proton-translocating $\mathbf{P_R} \rightarrow \mathbf{F}$ transition may reasonably be envisioned to fall into such a category of reactions.

On the Free Energy of P_R Formation. The thermodynamics of the reaction where $\mathbf{P_R}$ is formed is of special interest. On the basis of quantum chemical calculations Blomberg et al. (*56*) concluded that the formation of $\mathbf{P_M}$ from compound **A** is nearly isergonic, which is consistent with the observation that this reaction is not associated with translocation of electrical charge across the membrane. If this reaction were strongly exergonic, the free energy would be lost as heat. The same argument may be applied to formation of $\mathbf{P_R}$, since it is also not linked to translocation of charge perpendicular to the dielectric. However, let us consider the hypothetical case where $\mathbf{P_R}$ would be formed from the $\mathbf{P_M}$ state: this reaction would include the *apparently* very exergonic transfer

[4] The amino acid numbering refers to the sequence of subunit I of bovine cytochrome oxidase.

of an electron from Fe_a ($E_{m,7} \sim 0.35$ V) to the neutral tyrosine radical or to Cu_B(III) in the binuclear site, both electron acceptors having nominal E_m values (in water) well above 0.8 V (*73*). Although this electron transfer is probably accompanied by *local* proton transfer *within* the binuclear site in both cases (Figure 6), the negative charge of the binuclear center as a whole would be increased. The absence of any membrane potential generation is consistent with electron transfer from Fe_a to the binuclear center occurring parallel to the membrane plane (*14*, *38*), but this finding also shows that there is no significant compensation of the additional negative charge in the center from the surroundings on the time scale of $\mathbf{P_R}$ formation. As for example pointed out by Rich et al. (*74*), the free energy of placing an electrical charge into a low-dielectric site is considerable, and this would be expected to lower the E_m value of the electron acceptor in the binuclear center. Although it is difficult to evaluate the magnitude of this effect, it nevertheless provides a reasonable foundation for the idea that the formation of $\mathbf{P_R}$ is not a highly driven reaction thermodynamically, despite the very high nominal driving force. In this way, the free energy of the intrinsically exergonic proton uptake into the binuclear site during the conversion of $\mathbf{P_R}$ to **F** may be used to do useful work, i.e., by linkage of this reaction to translocation of a proton across the dielectric, as discussed above.

The above implies, of course, that the formation of $\mathbf{P_R}$ from $\mathbf{P_M}$ would not be very far from equilibrium, and this is supported quite independently by results from the reversal of the oxygen reaction in mitochondria at high $\Delta\mu_{H^+}$. In such conditions, Wikström (*9*) showed that $\mathbf{P_M}$ was formed from **F** at an apparent E_m of 0.375 V and an extramitochondrial pH of 7.7. This reaction would presumably first involve formation of $\mathbf{P_R}$ from **F** driven by reversal of the proton pump at high $\Delta\mu_{H^+}$, with subsequent transfer of an electron from $\mathbf{P_R}$ via Fe_a and cytochrome *c* to the redox buffer, yielding $\mathbf{P_M}$. Since the $\mathbf{P_R} \rightarrow \mathbf{P_M}$ transition would not by itself be linked to translocation of electrical charge across the dielectric, and the transfer of the electron to the redox buffer from the binuclear site only takes place across ca. one-third of the dielectric (*71*), it again follows that this transition cannot be strongly driven thermodynamically.

CONCLUSIONS

In the reaction of the fully reduced cytochrome *c* oxidase with O_2 the primary formation of a heme−oxygen adduct (compound **A**) is followed by electron transfer from heme *a* to the binuclear site. This creates the $\mathbf{P_R}$ intermediate at this site with optical as well as EPR properties quite distinct from intermediate **F**, which is formed subsequently. The optical spectrum of $\mathbf{P_R}$ and its unusual EPR spectrum suggest that the structure of the binuclear center is Fe(IV)═O Cu(II), probably with an OH^- ligand on the copper ion. The changed optical and EPR properties of **F** are consistent with an Fe(IV)═O Cu(II) structure, where the copper OH^- ligand may have been protonated to water, allowing for strong hydrogen bonding and exchange coupling between the heme iron and the copper sites. The $\mathbf{P_R}$ state of the binuclear center is considered to be electrostatically "charged", so that the electron transfer that creates it is nearly isoergonic. The charged $\mathbf{P_R}$ state relaxes to **F** with net uptake of a proton to the binuclear center from the *N*-side of the membrane, and this drives the first step of proton translocation across the membrane in the oxidative part of the catalytic cycle.

ACKNOWLEDGMENT

We thank Örjan Hansson and Tore Vänngård for access to their unpublished results.[3] We also thank Pekka Pihkala and Matti Lehtinen for their skilled assistance with design and construction of equipment.

REFERENCES

1. Wikström, M. (1977) *Nature 266*, 271−273.
2. Babcock, G. T., and Wikström, M. (1992) *Nature 356*, 301−309.
3. Ferguson-Miller, S., and Babcock, G. T. (1996) *Chem. Rev. 96*, 2889−2907.
4. Babcock, G. T. (1999) *Proc. Natl. Acad. Sci. U.S.A. 96*, 12971−12973.
5. Chance, B., Saronio, C., and Leigh, J. S. (1975) *J. Biol. Chem. 250*, 9226−9237.
6. Proshlyakov, D. A., Pressler, M. A., and Babcock, G. T. (1998) *Proc. Natl. Acad. Sci. U.S.A. 95*, 8020−8025.
7. Kitagawa, T., and Ogura, T. (1996) *Prog. Inorg. Chem. 45*, 431−480.
8. Fabian, M., Wong, W. W., Gennis, R. B., and Palmer, G. (1999) *Proc. Natl. Acad. Sci. U.S.A. 96*, 13114−13117.
9. Wikström, M. (1981) *Proc. Natl. Acad. Sci. U.S.A. 78*, 4051−4054.
10. Wrigglesworth, J. M. (1984) *Biochem. J. 217*, 715−719.
11. Vygodina, T., and Konstantinov, A. A. (1989) *Biochim. Biophys. Acta 973*, 390−398.
12. Weng, L., and Baker, G. M. (1991) *Biochemistry 30*, 5727−5733.
13. Fabian, M., and Palmer, G. (1995) *Biochemistry 34*, 1534−1540.
14. Ostermeier, C., Harrenga, A., Ermler, U., and Michel, H. (1997) *Proc. Natl. Acad. Sci. U.S.A. 94*, 10547−10553.
15. Gennis, R. B. (1998) *Biochim. Biophys. Acta 1365*, 241−248.
16. Proshlyakov, D. A., Pressler, M. A., DeMaso, C., Leykam, J. F., DeWitt, D. L., and Babcock, G. T. (2000) *Science 290*, 1588−1591.
17. Hill, B. C. (1991) *J. Biol. Chem. 266*, 2219−2226.
18. Hill, B. C. (1994) *J. Biol. Chem. 269*, 2419−2425.
19. Han, S., Ching, Y. C., and Rousseau, D. L. (1990) *Proc. Natl. Acad. Sci. U.S.A. 87*, 2491−2495.
20. Morgan, J. E., Verkhovsky, M. I., and Wikström, M. (1996) *Biochemistry 35*, 12235−12240
21. Sucheta, A., Szundi, I., and Einarsdóttir, Ó. (1998) *Biochemistry 37*, 17905−17914.
22. Orii, Y. (1988) *Ann. N.Y. Acad. Sci. 550*, 105−117.
23. Han, S., Takahashi, S., and Rousseau, D. L. (2000) *J. Biol. Chem. 275*, 1910−1919.
24. Ogura, T., Hirota, S., Proshlyakov, D. A., Shinzawa-Itoh, K., Yoshikawa, S., and Kitagawa, T. (1996) *J. Am. Chem. Soc. 118*, 5443−5449.
25. Hansson, Ö., Karlsson, B., Aasa, R., Vänngård, T., and Malmström, B. G. (1982) *EMBO J. 1*, 1295−1297.
26. Malmström, B. G. (1982) *Annu. Rev. Biochem. 51*, 21−59.
27. Malmström, B. G. (1993) *Acc. Chem. Res. 26*, 332−338.
28. Blair, D. F., Witt, S. N., and Chan, S. I. (1985) *J. Am. Chem. Soc. 107*, 7389−7399.
29. Hartzell, C. R., and Beinert, H. (1974) *Biochim. Biophys. Acta 368*, 318−338.
30. Baker, G. M., Noguchi, M., and Palmer, G. (1987) *J. Biol. Chem. 262*, 595−604.
31. Clore, G. M., Andreasson, L.-E., Karlsson, B., Aasa, R., and Malmström, B. G. (1980) *Biochem. J. 185*, 139−154.
32. Verkhovsky, M. I., Morgan, J. E., Puustinen, A., and Wikström, M. (1996) *Biochemistry 35*, 16241−16246.
33. Provincer, S. W., and Vogel, R. H. (1983) in *Progress in Scientific Computing* (Deuflhard, P., and Hairer, E., Eds.) Vol. 2, pp 304−319, Birkhäuser, Boston, MA.

34. Karlsson, B., Aasa, R., Vänngård, T., and Malmström, B. G. (1981) *FEBS Lett. 131*, 186−188.
35. Powers, L., Lauraeus, M., Reddy, K. S., Chance, B., and Wikström, M. (1994) *Biochim. Biophys. Acta 1183*, 504−512.
36. Malmström, B. G., and Vänngård, T. (1960) *J. Mol. Biol. 2*, 118−124.
37. Peisach, J., and Blumberg, W. E. (1974) *Arch. Biochem. Biophys. 165*, 691−710.
38. Yoshikawa, S., Shinzawa-Itoh, K., Nakashima, R., Yaono, R., Yamashita, E., Inoue, N., Yao, M., Fei, M. J., Libeu, C. P., Mizushima, T., Yamaguchi, H., Tomizaki, T., and Tsukihara, T. (1998) *Science 280*, 1723−1729.
39. Surerus, K. K., Oertling, W. A., Fan, C., Gurbiel, R. J., Einarsdóttir, Ó., Antholine, W. E., Dyer, R. B., Hoffman, B. M., Woodruff, W. H., and Fee, J. A. (1992) *Proc. Natl. Acad. Sci. U.S.A. 89*, 3195−3199.
40. Karpefors, M., Ädelroth, P., Aagaard, A., Smirnova, I. A., and Brzezinski, P. (1999) *Isr. J. Chem. 39*, 427−437.
41. Hallén, S., and Nilsson, T. (1992) *Biochemistry 31*, 11853−11859.
42. Mitchell, R., Mitchell, P., and Rich, P. R. (1992) *Biochim. Biophys. Acta 811*, 188−191.
43. Jasaitis, A., Verkhovsky, M. I., Morgan, J. E., Verkhovskaya, M. L., and Wikström, M. (1999) *Biochemistry 38*, 2697−2706.
44. Wittenberg, B. A., and Wittenberg, J. B. (1989) *Annu. Rev. Physiol. 51*, 857−878.
45. Gnaiger, E., Méndez, G., and Hand, S. C. (2000) *Proc. Natl. Acad. Sci. U.S.A. 97*, 11080−11085.
46. Jasaitis, A., Backgren, C., Morgan, J. E., Puustinen, A., Verkhovsky, M. I. and Wikström, M. (2001) *Biochemistry* (submitted for publication).
47. Wikström, M., Krab, K., and Saraste, M. (1981) *Cytochrome Oxidase−a synthesis*, pp 129−131, Academic Press, London and New York.
48. Zickermann, I., Anemüller, S., Richter, O.-M. H., Tautu, O. S., Link, T. A., and Ludwig, B. (1996) *Biochim. Biophys. Acta 1277*, 93−102.
49. Benecky, M. J., Frew, J. E., Scowen, N., Jones, P., and Hoffman, B. M. (1993) *Biochemistry 32*, 11929−11933.
50. Bill, E., Ding, X.-Q., Bominaar, E. L., Trautwein, A. X., Winkler, H., Mandon, D., Weiss, R., Gold, A., Jayaraj, K., and Hatfield, W. E. (1990) *Eur. J. Biochem. 188*, 665−672.
51. Mandon, D., Weiss, R., Jayaraj, K., Gold, A., Bill, E., Terner, J., and Trautwein (1992) *Inorg. Chem. 31*, 4404−4409.
52. Rutter, R., Hager, L. P., Dhonau, H., Hendrich, M., Valentine, M., and Debrunner, P. G. (1984) *Biochemistry 23*, 6809−6816.
53. Schultz, C. E., Devaney, P. W., Winkler, H., Debrunner, P. G., Doan, N., Chang, R., Rutter, R., and Hager, L. P. (1978) *FEBS Lett. 103*, 102−105.
54. Bencini, A., and Gatteschi, D. (1984) *Mol. Phys. 54*, 969−977.
55. Hulliger, J. (1987) *Mol. Phys. 60*, 97−6110.
56. Blomberg, M. R. A., Siegbahn, P. E. M., Babcock, G. T., and Wikström, M. (2000) *J. Am. Chem. Soc. 122*, 12848−12858.
57. Verkhovsky, M. I., Morgan, J. E., and Wikström, M. (1994) *Biochemistry 33*, 3079−3085.
58. Karpefors, M., Ädelroth, P., Namslauer, A., Zhen, Y., and Brzezinski, P. (2000) *Biochemistry 39*, 14664−14669.
59. Michel, H. (1998) *Proc. Natl. Acad. Sci. U.S.A. 95*, 12819−12824.
60. Wikström, M. (2000) *Biochim. Biophys. Acta 1458*, 188−198.
61. Pillbrow, J. (1990) *Transition Ion Electron Paramagnetic Resonance*, p 222, Oxford University Press, New York.
62. Fabian, M., and Palmer, G. (2001) *Biochemistry* (in press).
63. Oliveberg, M., and Malmström, B. G. (1991) *Biochemistry 30*, 7053−7057.
64. Morgan, J. E., Li, P. M., Jang, D.-J., El-Sayed, M. A., and Chan, S. I. (1989) *Biochemistry 28*, 6975−6983.
65. Brzezinski, M., and Malmström, B. G. (1987) *Biochim. Biophys. Acta 894*, 29−38.
66. Ädelroth, P., Svensson, Ek, M., Mitchell, D. M., Gennis, R. B., and Brzezinski, P. (1997) *Biochemistry 36*, 13824−13829.
67. Brzezinski, P., and Ädelroth, P. (1998) *J. Bioenerg. Biomembr. 30*, 99−107.
68. Rich, P. R. (1995) *Aust. J. Plant Physiol. 22*, 479−486.
69. Morgan, J. E., Verkhovsky, M. I., and Wikström, M. (1994) *J. Bioenerg. Biomembr. 26*, 599−608.
70. Michel, H. (1999) *Biochemistry 38*, 15129−15140.
71. Verkhovsky, M. I., Jasaitis, A., Verkhovskaya, M. L., Morgan, J. E., and Wikström, M. (1999) *Nature 400*, 480−483.
72. Austin, R. H., Beeson, K. W., Eisenstein, L., Frauenfelder, H., and Gunsalus, I. C. (1975) *Biochemistry 14*, 5355−5373.
73. Tommos, C., and Babcock, G. T. (2000) *Biochim. Biophys. Acta 1458*, 199−219.
74. Rich, P. R., Meunier, B., Mitchell, R., and Moody, A. J. (1996) *Biochim. Biophys. Acta 1275*, 91−95.

BI010246W